OPEN ACCESS



Converging on the Cepheid Metallicity Dependence: Implications of Nonstandard Gaia Parallax Recalibration on Distance Measures

Louise Breuval^{1,18}, Gagandeep S. Anand², Richard I. Anderson³, Rachael Beaton², Anupam Bhardwaj⁴, Stefano Casertano², Gisella Clementini⁵, Mauricio Cruz Reyes³, Giulia De Somma^{6,7,8}, Martin A. T. Groenewegen⁹, Caroline D. Huang^{10,19}, Pierre Kervella^{11,12}, Saniya Khan³, Lucas M. Macri¹³, Marcella Marconi⁶, Javier H. Minniti¹⁴, Adam G. Riess^{2,14}, Vincenzo Ripepi⁶, Martino Romaniello¹⁵, Daniel Scolnic¹⁶, Erasmo Trentin⁶, Piotr Wielgórski¹⁷, and Wenlong Yuan¹⁴ ¹ European Space Agency (ESA), ESA Office, Space Telescope Science Institute, 3700 San Martin Drive, Baltimore, MD 21218, USA; lbreuval@stsci.edu Space Telescope Science Institute, 3700 San Martin Drive, Baltimore, MD 21218, USA ³ Institute of Physics, École Polytechnique Fédérale de Lausanne (EPFL), Observatoire de Sauverny, 1290 Versoix, Switzerland Inter-University Centre for Astronomy and Astrophysics (IUCAA), Post Bag 4, Ganeshkhind, Pune 411 007, India 5 INAF, Osservatorio di Astrofisica e Scienza dello Spazio di Bologna, Via Piero Gobetti 93/3, 40129 Bologna, Italy INAF—Osservatorio Astronomico di Capodimonte, Via Moiariello 16, 80131 Napoli, Italy ⁷ INAF—Osservatorio Astronomico d'Abruzzo, Via Maggini sn, 64100 Teramo, Italy ⁸ Istituto Nazionale di Fisica Nucleare (INFN), Sezione di Napoli, Compl. Univ. di Monte S. Angelo, Edificio G, Via Cinthia, I-80126 Napoli, Italy Koninklijke Sterrenwacht van België, Ringlaan 3, B-1180 Brussels, Belgium ¹⁰ Center for Astrophysics | Harvard & Smithsonian, 60 Garden Street, Cambridge, MA 02138, USA 11 LIRA, Observatoire de Paris, Université PSL, Sorbonne Université, Université Paris Cité, CY Cergy Paris Université, CNRS, 5 place Jules Janssen, 92195 Meudon, France ¹² French-Chilean Laboratory for Astronomy, IRL 3386, CNRS and U. de Chile, Casilla 36-D, Santiago, Chile ¹³ Department of Physics & Astronomy, College of Sciences, University of Texas Rio Grande Valley, 1201 W University Drive, Edinburg TX 78539, USA Department of Physics and Astronomy, Johns Hopkins University, Baltimore, MD 21218, USA European Southern Observatory, Karl-Schwarzschild-Strasse 2, 85478 Garching bei München, Germany
Department of Physics, Duke University, Durham, NC 27708, USA ¹⁷ Nicolaus Copernicus Astronomical Center, Polish Academy of Sciences, Bartycka 18, 00-716 Warszawa, Poland Received 2025 July 16; revised 2025 September 23; accepted 2025 September 25; published 2025 November 19

Abstract

By comparing Cepheid brightnesses with geometric distance measures including Gaia EDR3 parallaxes, most recent analyses conclude metal-rich Cepheids are brighter, quantified as $\gamma \sim -0.2$ mag dex $^{-1}$. While the value of γ has little impact on the determination of the Hubble constant in contemporary distance ladders (due to the similarity of metallicity across these ladders), γ plays a role in gauging the distances to metal-poor dwarf galaxies like the Magellanic Clouds and is of considerable interest in testing stellar models. Recently, B. F. Madore & W. L. Freedman (hereafter MF25) recalibrated Gaia EDR3 parallaxes by adding to them a magnitude offset to match certain historic Cepheid parallaxes, which otherwise differ by $\sim 1.6\sigma$. A calibration that adjusts Gaia parallaxes by applying a magnitude offset (i.e., a multiplicative correction in parallax) differs significantly from the Gaia Team's calibration, which is additive in parallax space—especially at distances much closer than 1 kpc or beyond 10 kpc, outside the $\sim 2-3$ kpc range on which the MF25 calibration was based. The MF25 approach reduces γ to zero. If broadly applied, it places nearby cluster distances like the Pleiades too close compared to independent measurements, while leaving distant quasars with negative parallaxes. We conclude that the MF25 proposal for Gaia calibration and $\gamma \sim 0$ produces farther-reaching consequences, many of which are strongly disfavored by the data.

Unified Astronomy Thesaurus concepts: Cepheid variable stars (218); Distance measure (395); Parallax (1197); Metallicity (1031)

1. Introduction

The dependence of the Cepheid period–luminosity (P–L) relation on metallicity is astrophysical in nature, is quantified as γ (in mag dex⁻¹), and is crucial when using Cepheid brightnesses to determine their distances. Since the time of the final result of the HST Key Project (R. C. J. Kennicutt et al. 1998; W. L. Freedman et al. 2001), this term was found to be

Original content from this work may be used under the terms of the Creative Commons Attribution 4.0 licence. Any further distribution of this work must maintain attribution to the author(s) and the title of the work, journal citation and DOI.

negative, indicating that at fixed period and color, metal-rich Cepheids are intrinsically brighter. W. L. Freedman et al. (2001) write: "Published empirical values for the index γ range from 0 to -1.3 mag dex⁻¹ (with most values between 0 and -0.4) [...] Other recent studies conclude that a metallicity effect is extant, and all of the empirical studies agree on the sign, if not the magnitude of the effect. Considering all of the evidence currently available and the (still considerable) uncertainties, we therefore adopt $\gamma = -0.2 \pm 0.2$ mag dex⁻¹, approximately the midrange of current empirical values, and correct our Cepheid distances accordingly." Although its exact value is still debated, the community has now reached a broad, though not unanimous, consensus on the negative sign and on the value of this effect: $\gamma \sim -0.2$ mag dex⁻¹ with variations of about ± 0.1 mag dex⁻¹ depending on the study (see Figure 1).

¹⁸ ESA Research Fellow.

¹⁹ NSF Astronomy and Astrophysics Postdoctoral Fellow.

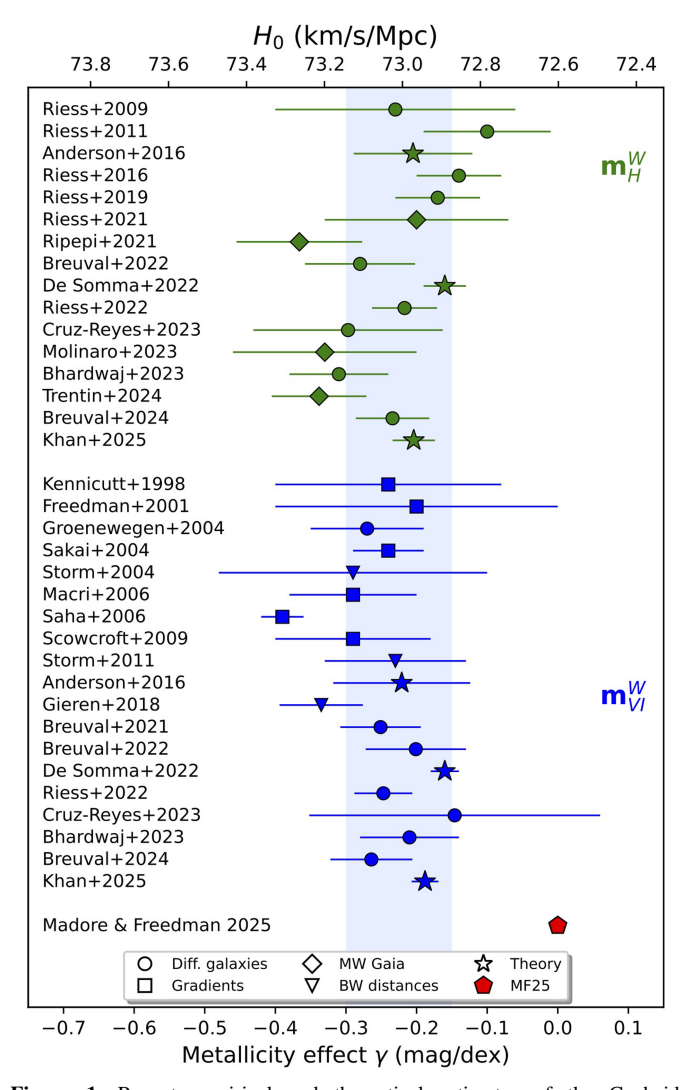


Figure 1. Recent empirical and theoretical estimates of the Cepheid metallicity dependence γ from the literature in the m_H^W and m_{VI}^W Wesenheit indices. A few analyses were excluded from this plot (e.g., W. L. Freedman & B. F. Madore 2011; P. Wielgórski et al. 2017; K. A. Owens et al. 2022) due to issues that were identified and discussed in L. Breuval et al. (2022). The blue band shows broad agreement between $\gamma \sim -0.15$ and -0.30 mag dex⁻¹. The methods labeled with different shapes include comparison between P-L relations in different galaxies, metallicity gradients, Milky Way Cepheids with Gaia EDR3 parallaxes, Baade-Wesselink distances, and theoretical predictions. The red point indicates the $\gamma \sim 0$ multiwavelength result by MF25, based on a variety of methods. The metallicity dependence γ in the m_H^W Wesenheit magnitude and the Hubble constant H_0 are related as follows: γ shifts the luminosity of Cepheids which show the largest metallicity difference with respect to Cepheids in SNIa hosts (i.e., in the SH0ES distance ladder, the metal-poor LMC, and SMC). This luminosity difference directly translates into a shift in H_0 . We note that the H_0 values represented on the top x-axis are not actually measured in the quoted references but are derived from H0DN Collaboration et al. (2025).

A metallicity dependence of Cepheid pulsation properties is theoretically expected. Stellar evolution models predict that, at fixed mass, metal-rich Cepheids are slightly fainter than their metal-poor counterparts (V. Castellani et al. 1992; G. Bono et al. 2000a), with helium abundance showing the opposite effect. In contrast, stellar pulsation models (G. Bono et al. 2000b; M. Marconi et al. 2005; R. I. Anderson et al. 2016; G. De Somma et al. 2022; S. Khan et al. 2025) predict that an increase in metallicity shifts the instability strip to redder colors at constant stellar mass, as the enhanced opacity reduces

pulsation driving in the hydrogen ionization zone (see G. Bono et al. 1999 for details). Conversely, a higher helium abundance shifts the instability strip in the opposite direction (G. Fiorentino et al. 2002; M. Marconi et al. 2005). These dependencies directly affect the P–L and Period–Wesenheit relations, and all recent models consistently predict that, at fixed period and color, metal-rich Cepheids are intrinsically brighter than metal-poor ones ($\gamma < 0$). We further note that the modeled atmosphere results presented in B. F. Madore et al. (2025b) do not change the above scenario, because a metallicity dependence is already expected in bolometric magnitudes as an effect of the pulsation mechanism physics and is not only an atmospheric phenomenon.

In order to calibrate Cepheid distances in the Milky Way, to estimate the metallicity dependence of the P-L relation, and to measure extragalactic distances and ultimately the local value of the Hubble Constant (H_0) , many recent empirical studies (e.g., L. Breuval et al. 2021, 2022; A. G. Riess et al. 2021; X. Zhou & X. Chen 2021; K. A. Owens et al. 2022; A. G. Riess et al. 2022a; V. Ripepi et al. 2022, 2023; A. Bhardwaj et al. 2023, 2024; M. Cruz Reyes & R. I. Anderson 2023; E. Trentin et al. 2024) rely on Gaia Early Data Release 3 (EDR3), which provides stellar parallaxes for over 1.5 billion sources with unprecedented accuracy and completeness (Gaia Collaboration et al. 2021). Gaia EDR3 parallaxes require additional calibration at the level of $\sim 20 \,\mu as$. A primary source of calibration comes from Gaia EDR3 astrometry of quasars, which reveals parallaxes that are negative by a few tens of microarcseconds. Additional calibration comes from stars in the Large Magellanic Cloud (LMC), with extension to brighter magnitudes from physical pairs. Based on an extensive, simultaneous analysis of this data, L. Lindegren et al. (2021a, hereafter L21) provide a calibration or parallax offset correction (hereafter ϖ_{L21}), an angular term that is a function of magnitude, color, and ecliptic latitude. This parallax correction—which produces the most accurate results—involves subtracting²⁰ a value in angular units derived by the provided function, ²¹ and has been corroborated by independent studies (e.g., M. A. T. Groenewegen 2021; J. Maíz Apellániz et al. 2021). Various works have investigated the need for an additional offset in the brighter range of magnitudes (G < 10 mag) where the L21 analysis has limited sampling (A. Bhardwaj et al. 2021; C. Fabricius et al. 2021; Y. Huang et al. 2021; F. Ren et al. 2021; K. G. Stassun & G. Torres 2021; E. Vasiliev & H. Baumgardt 2021; J. C. Zinn 2021; S. Khan et al. 2023). For a sample of 75 Milky Way Cepheids (G < 8 mag), A. G. Riess et al. (2021) find a best-fit residual offset (hereafter $\varpi_{ ext{offset}}$) after application of the L21 correction, of $\varpi_{\text{offset}} = -14 \pm 6 \,\mu\text{as}$, in the sense that L21 slightly overcorrects parallaxes. This step does not depend on any external parallax reference, and is based only on minimizing the P-L dispersion. Other independent studies have obtained similar values (M. Cruz Reyes & R. I. Anderson 2023; E. Trentin et al. 2024; H. Wang et al. 2024, with ϖ_{offset} = $-19 \pm 3 \,\mu \mathrm{as}$, $\varpi_{\mathrm{offset}} = -15 \pm 3 \,\mu \mathrm{as}$, and $\varpi_{\mathrm{offset}} < 0 \,\mu \mathrm{as}$, respectively). Overall, adopting the L21 parallax calibration $\varpi_{\rm L21}$ as well as a $\varpi_{\rm offset} = -14 \,\mu{\rm as}$ counter-correction for

²⁰ L21: "Regarded as a systematic correction to the parallax, the bias function Z5 or Z6 should be subtracted from the value (parallax) given in the archive. Python implementations of both functions are available in the Gaia web pages."

https://www.cosmos.esa.int/web/gaia/edr3-code

Gaia Collaboration (L21)	B. F. Madore & W. L. Freedman (2025)
Correction in Parallax Space	Correction in Magnitude Space $(m-M)_{\text{corr}} = (m-M)_{\text{Gaia EDR3}} - 0.26$
Additive Parallax Offset $\varpi_{\text{corr}} = \varpi_{\text{Gaia EDR3}} + \text{L21}$	Equiv. to Multiplicative Parallax Offset $\varpi_{\rm corr} = 1.127 \times \varpi_{\rm Gaia\ EDR3}$

These two different corrections have consequences on distance to Pleiades, quasar parallaxes, and the inferred measurement of H_0

Cepheids results in a metallicity dependence γ consistent with -0.2 ± 0.1 mag dex⁻¹.

Instead of individual Cepheids, Milky Way open clusters have been used to achieve better astrometric precision for the Cepheids they host, because their parallaxes can be averaged over a large number of stars (R. I. Anderson et al. 2013; L. Breuval et al. 2020; A. G. Riess et al. 2022a; M. Cruz Reyes & R. I. Anderson 2023). However, since cluster members are located in the same region of the sky, their parallaxes are highly correlated. As a result, even though the statistical uncertainty of a mean cluster parallax can be as low as $2 \mu as$, the cluster parallax precision is dominated by the angular covariance, currently estimated to \sim 7 μ as (J. Maíz Apellániz et al. 2021; E. Vasiliev & H. Baumgardt 2021). The other advantage of using cluster Cepheids is that cluster members are generally fainter (G > 13 mag), and thus have good overlap with the magnitude and color range of the L21 calibration, reducing the size or need for residual parallax offsets. A. G. Riess et al. (2022a) and M. Cruz Reyes & R. I. Anderson (2023) used cluster Cepheids and found no evidence of residual offset beyond the L21 correction in this magnitude range. Similarly, H. Wang et al. (2024) adopt the largest sample of Milky Way cluster Cepheids to date along with their mean Gaia EDR3 parallaxes and find a residual parallax offset consistent with zero for cluster members. In conclusion, using cluster Cepheids with only the L21 correction returns similar results compared with using field Cepheids with L21 and the additional $-14 \mu as$: both yield a metallicity dependence γ consistent with -0.2 mag dex⁻¹, and a distance modulus to the LMC in excellent agreement with the geometric distance by G. Pietrzyński et al. (2019).

B. F. Madore & W. L. Freedman (2025, hereafter MF25) offer a very different approach to the preceding analyses (see Table 1). In MF25, the earlier generation of parallax measurements from the Hubble Space Telescope (HST) Fine Guidance Sensor (FGS) from G. F. Benedict et al. (2007, hereafter B07) is used to recalibrate those from Gaia EDR3 and to conclude that metallicity has no statistically significant effect, $\gamma \sim 0$, on the Cepheid P–L (and Period–Wesenheit) relation across various wavelengths. As we will discuss in Section 3, this approach would decrease the Hubble constant by about $0.4 \,\mathrm{km \, s^{-1} \, Mpc^{-1}}$. While the MF25 conclusion, $\gamma \sim 0$, is drawn from a broad data set and multiple tests, several aspects warrant a critical examination to assess the robustness of this claim. In particular, instead of applying the additive L21 calibration in parallax space, MF25 subtract a fixed magnitude of 0.26 mag from each Cepheid distance modulus to produce a specific P-L scatter when their Gaia sample is combined with older parallax measures of 10

Cepheids from B07. An offset in magnitude space acts as a multiplicative correction in parallax, which based on the way Gaia parallaxes are measured (closed phase and imperfect basic angle monitor due to thermal variations and geometric distortions producing small astrometric shifts) would not be the expected mathematical operation to calibrate any Gaia parallaxes (empirical studies of the residual parallax bias as a function of apparent magnitude, e.g., S. Khan et al. 2023, and references therein, rule out a simple multiplicative model). The MF25 calibration is applied to the distance modulus:

$$(m-M)_{\text{MF25}} = (m-M)_0 - 0.26,$$
 (1)

where the initial distance modulus is defined as $(m-M)_0=10-5\log(\varpi_{\text{Gaia}\,\text{EDR3}})$ with $\varpi_{\text{Gaia}\,\text{EDR3}}$ the Gaia EDR3 parallax. As a consequence, the MF25 approach is equivalent to using a parallax ϖ_{MF25} , where:

$$\varpi_{\text{MF25}} = 1.127 \ \varpi_{\text{Gaia EDR3}}.$$
(2)

On the other hand, the parallax calibration recommended by the Gaia team is:

$$\varpi_{\text{Gaia,corr}} = \varpi_{\text{Gaia EDR3}} + \varpi_{\text{L21}},$$
(3)

where ϖ_{L21} is the L21 correction. These two approaches are summarized in Table 1.

In Section 2, we inspect the multiple tests carried out by MF25 and, where possible, point out more up-to-date data sets available for the same analyses, ensuring consistency with recent developments in the field. While a multiplicative and additive calibration may nearly coincide at some parallax, they will be unequal over a wider range. Therefore, in Section 3, we discuss how the MF25 Gaia calibration would perform nearby and far away, as well as for the local value of the Hubble Constant. We conclude with a discussion in Section 4.

2. Revisiting the MF25 Finding of a Null Cepheid Metallicity Dependence

A departure from most studies in the last $\sim\!25\,\mathrm{yr}$ to claim that the metallicity dependence is consistent with zero, as in MF25, requires strong evidence and identifying why nearly all recent studies (Figure 1) find a systematically negative dependence. In this section we investigate the methods employed in MF25 that lead to the conclusion of a null metallicity dependence.

2.1. The MF25 Recalibration of Gaia EDR3 Parallaxes

The key to the difference in conclusion reached in MF25 concerning γ lies in the unusual treatment of Gaia EDR3 parallaxes in that work. Most contemporary studies treat Gaia EDR3 as a generational improvement in parallax precision and scope, warranting replacement of all prior measurements. After applying the recommended L21 calibration function, which is additive in parallax and of size $\sim\!20\,\mu{\rm as}$, the systematic accuracy in the well-calibrated region is estimated at "a few microarcseconds." As evidence, L21 show a measure of the LMC parallax consistent with the expectation from detached eclipsing binaries (hereafter DEBs, G. Pietrzyński et al. 2019) to within a few microarcseconds and the AGN catalog has a mean parallax of 0.5 $\mu{\rm as}$.

In contrast, MF25 identify an offset between (1) the Cepheid P–L relation for Gaia EDR3 parallaxes of Cepheids in clusters before application of the L21 calibration term, and (2) the

Cepheid P-L relation for 10 nearby Cepheids with previous generation HST FGS parallaxes from B07. MF25 discard the L21 parallax calibration and apply a magnitude offset of 0.26 mag to each Cepheid distance modulus, so that the P-L dispersion of the cluster Cepheid sample and HST FGS sample combined matches the P-L dispersion obtained in the LMC.²² The B07 parallaxes are an order of magnitude less precise (200-300 µas) than those from Gaia EDR3, allowing meaningful parallax measurements for only the nearest ~ 10 Cepheids, but also a factor of 10 less precise than Gaia's residual parallax bias, which disqualifies them from providing strong constraints. Additionally, the magnitude range of Cepheids in B07 is too bright for good Gaia parallaxes, precluding an immediate comparison in parallax space, hence MF25 used P–L relations instead. Doing the comparison in magnitude/P-L relation space, as in MF25, brings additional complications and leads to the interpretation of Gaia's systematics as a multiplicative term, which would have wide-ranging consequences that were not considered in MF25 and are addressed here. Finally, we note that B07 HST FGS parallaxes are infrequently used in current P-L calibrations, as they have been superseded by Gaia EDR3 parallaxes. For example, A. Gallenne et al. (2025) show that the P-L relation based on B07 parallaxes yields inaccurate distances compared to precise geometric measurements. Therefore, it might seem questionable to require the astrometrically more accurate and widely tested Gaia EDR3 parallaxes to match the less accurate.

Adopting the MF25 correction rather than the L21 calibration assumes three elements: (1) that the 1.6σ difference between the Gaia EDR3 and the B07 samples is significant and warrants a parallax recalibration, (2) that any parallax inaccuracy lies with Gaia EDR3 rather than the 10 HST FGS parallaxes from B07, and (3) that matching the LMC geometric distance without a Cepheid metallicity term is preferable. Thus, bringing Gaia EDR3 parallaxes of clusters hosting Cepheids into better agreement with the HST FGS parallax sample reduces the metallicity term γ to zero, but with what consequences (see Section 3)?

2.2. Reproducing the Initial Measurement by MF25

In this section, we adopt the same data sets and assumptions as in MF25 to attempt a reproduction of the reported results. That study identified 13 cluster Cepheids in the Milky Way based on common proper motions of member stars. Although a much larger sample of >30 cluster Cepheids is available in the literature (e.g., R. I. Anderson et al. 2013; L. Breuval et al. 2020; A. G. Riess et al. 2022a; M. Cruz Reyes & R. I. Anderson 2023; H. Wang et al. 2024), the analysis in MF25 is carried out in the Spitzer [3.6 μ m] filter in order to minimize the effects of interstellar absorption and width of the instability strip. In that filter, only 37 Milky Way Cepheids have available photometry from A. J. Monson et al. (2012), among which only 30% are in clusters, thereby significantly limiting the usable sample size. Among the 13 cluster Cepheids retained in MF25, EV Sct and CS Vel were explicitly excluded and do not appear in their Figure 3, therefore only 11 cluster Cepheids are used. In MF25's Table 1, the Cepheid WZ Sgr is associated with the open cluster "Turner 2." MF25 note in their Appendix A.9. that "the reality of Turner 2 as a bona fide cluster is questionable." This cluster appears in E. L. Hunt & S. Reffert (2023) in the list of clusters reported in the literature that were not recovered using Gaia EDR3. Similarly, M. Cruz Reyes & R. I. Anderson (2023) performed a search for clusters in the vicinity of Cepheids and did not recover a cluster associated with WZ Sgr based on Gaia EDR3 astrometry. Turner 2 is listed in the N. V. Kharchenko et al. (2013) catalog but with only one star used to measure the radial velocity, and only 24 stars within a r_1 radius. It does not exist in other modern catalogs based on Gaia (T. Cantat-Gaudin et al. 2020; A. Castro-Ginard et al. 2022), is mentioned in D. G. Turner et al. (1993) under a different name ("C1814-191a"), and is described as a "sparse cluster." Since we cannot reproduce the mean parallax of this cluster with Gaia EDR3 parallaxes, we exclude it from our reanalysis. Following MF25, we fix the P-L slope to the LMC value (-3.31, V. Scowcroft et al. 2012, for 6 < P < 60 days) and we fit the P-L relation for the cluster Cepheid sample (N=10) from MF25, where the absolute magnitudes $M_{13.61}$

$$M_{[3.6]} = m_{[3.6]} - 0.203 E(B - V) - (m - M)_{0,\text{corr}}.$$
 (4)

Apparent magnitudes $m_{[3.6]}$ are from Table 4 in A. J. Monson et al. (2012), the distance moduli $(m-M)_{0, \text{ corr}}$ for each Cepheid are from Table 1 in MF25 and already include their 0.26 mag offset, and E(B-V) are from MF25 as well. A systematic error of 0.016 mag is included for the photometry error in $m_{[3.6]}$, and 0.06 mag errors are added in quadrature to absolute magnitude errors for the intrinsic width of the instability strip. We thus obtain:

$$M_{[3.6]} = -3.31 (\log P - 1) - (5.823 \pm 0.022),$$
 (5)

with $\sigma=0.071$ mag. This corresponds to the initial cluster Cepheid P–L relation as obtained in MF25, with the same pivot period (log $P_0=1$). We can compare it with that in the LMC to derive a first estimate of the metallicity dependence γ . In the LMC, using data from V. Scowcroft et al. (2012) with $E(B-V)=0.07\pm0.01$ mag, P<60 days, a fixed slope of -3.31 and a geometric distance to the LMC of $d=49.59\pm0.09\pm0.054$ kpc (G. Pietrzyński et al. 2019), we obtain:

$$M_{[3.6]} = -3.31 (\log P - 1) - (5.787 \pm 0.010).$$
 (6)

The difference in P–L intercept $(\Delta\beta)$ between the Milky Way clusters (Equation (5)) and the LMC sample (Equation (6)) is 0.036 ± 0.024 mag. For the Milky Way and LMC Cepheid metallicities, we adopt [Fe/H] = $+0.146\pm0.075$ and -0.407 ± 0.02 dex, respectively (L. Breuval et al. 2022; M. Romaniello et al. 2022). The metallicity effect γ is therefore defined as:

$$\gamma = \frac{\Delta \beta}{\Delta [\text{Fe/H}]} \tag{7}$$

and yields $\gamma = -0.06 \pm 0.05$ mag dex⁻¹. As MF25 conclude, this method suggests that the metallicity dependence of the P-L intercept is small and not significantly negative, contrary to what most empirical studies find. Instead of adding a 0.26 mag offset to match an expected dispersion, if MF25 had applied a slightly larger magnitude offset to exactly match the HST FGS

 $^{^{22}}$ MF25: "the data are fit to an a priori dispersion, rather than to a minimum dispersion. [...] We determine this offset only once (at 3.6 μ m), and next apply it equally to all other bands, without modification."

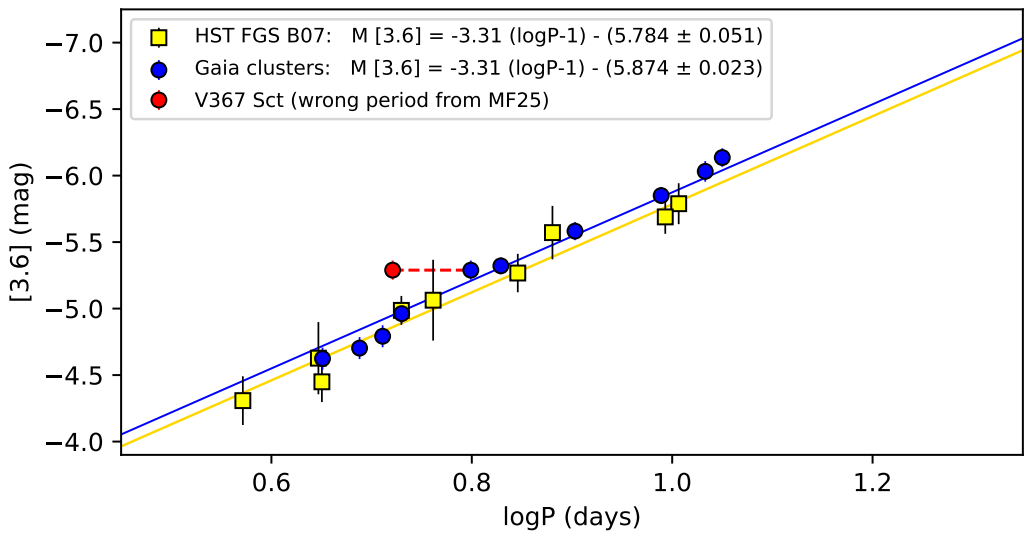


Figure 2. P-L relation for Milky Way cluster Cepheids (blue) as selected by MF25, after applying the corrections listed in Table 2, and for the HST FGS sample from B07 (yellow). The red point shows V367 Sct as plotted using MF25's incorrect period. The blue version uses the correct $\log P = 0.799$ value.

Table 2 Successive Updates of the Milky Way Cluster Cepheid P–L Relation, $M_{[3.6]} = \alpha (\log P - 1) + \beta$, from MF25

β	σ	γ	Comments
(mag)	(mag)	(mag dex^{-1})	
-5.823 ± 0.022	0.071	-0.06 ± 0.05	Initial MF25 calibration including 0.26 mag offset
-5.865 ± 0.024	0.078	-0.14 ± 0.05	Replace $(m - M)_{0, MF25}$ with Gaia EDR3 parallaxes + L21
-5.874 ± 0.023	0.080	-0.16 ± 0.05	Add V367 Sct with correct period

Note. Columns 1 and 2 give the P–L intercept and scatter, respectively, column 3 gives the inferred metallicity dependence γ and the last column describes the improvements corresponding to each row.

parallax P–L, a metallicity dependence $\gamma \sim 0$ would have been obtained. In the next section, we reevaluate the Milky Way Cepheid P–L relation and the metallicity dependence using better (see Table 2) and more modern data.

2.3. Updating the MF25 Measurement

Here, we adopt the same Cepheid sample as in MF25 with their Gaia EDR3 parallaxes taken from A. G. Riess et al. (2022a; or see M. Cruz Reyes & R. I. Anderson 2023; H. Wang et al. 2024) instead of the distance moduli with ad hoc calibration from MF25. These parallaxes include the L. Lindegren et al. (2021a) correction with no additional terms. MF25 claim that clusters "improve statistical precision by a factor of 16" compared to individual Cepheids. However, it should be noted that clusters only improve parallax precision by a factor of \sim 3, after accounting for an additional \sim 7 μ as term in the parallax error due to angular covariance (J. Maíz Apellániz et al. 2021; E. Vasiliev & H. Baumgardt 2021). These are included in the mean cluster parallax uncertainties. After inspecting the P-L diagram, we noticed that the cluster Cepheid V367 Sct (shown in red in Figure 2) appears as an outlier compared to the other well aligned data points, and that it was excluded from the P-L figures in MF25 without justification. For this Cepheid, MF25 adopt log P = 0.721 (see their Table 1) as in B. F. Madore & S. van den Bergh (1975). However, B. F. Madore et al. (1978) identify V367 Sct as a double-mode Cepheid and provide fundamental and first overtone periods of 6.29307 days (log P = 0.799) and

4.38466 days ($\log P = 0.642$), respectively. All recent studies use $\log P = 0.799$ as well (A. J. Monson et al. 2012; L. Breuval et al. 2020; X. Zhou & X. Chen 2021; A. G. Riess et al. 2022b; M. Cruz Reyes & R. I. Anderson 2023), which is the correct fundamental-mode pulsation period. In the following, we update the pulsation period of this Cepheid with $\log P = 0.799$.

The successive updates presented here are shown in Figure 3 and are listed in Table 2, where the first row is the original P–L relation obtained in the same conditions as MF25. Our best reevaluation of the Milky Way cluster Cepheid P–L relation is:

$$M_{[3.6]} = -3.31 (\log P - 1) - (5.874 \pm 0.023),$$
 (8)

with σ = 0.080 mag. It is represented in Figure 3 with a red circle. Assuming the same metallicities as in Section 2.2 and the same LMC P–L intercept of -5.787 ± 0.010 mag, we now obtain:

$$\gamma_{[3.6]} = -0.16 \pm 0.05 \text{ mag/dex},$$
 (9)

in good agreement with most estimates from the literature. The key difference here is a net, mean 0.05 mag difference between the MF25 and L. Lindegren et al. (2021a) calibration of Gaia parallaxes (see β values in Table 2), which represents about half the size of the metallicity effect between the Milky Way (MW) and the LMC (or the full size if the HST FGS parallaxes are assumed to define the reference).

We further note that MF25 claim that the results from L. Breuval et al. (2021, 2022) must be "extrapolated into the

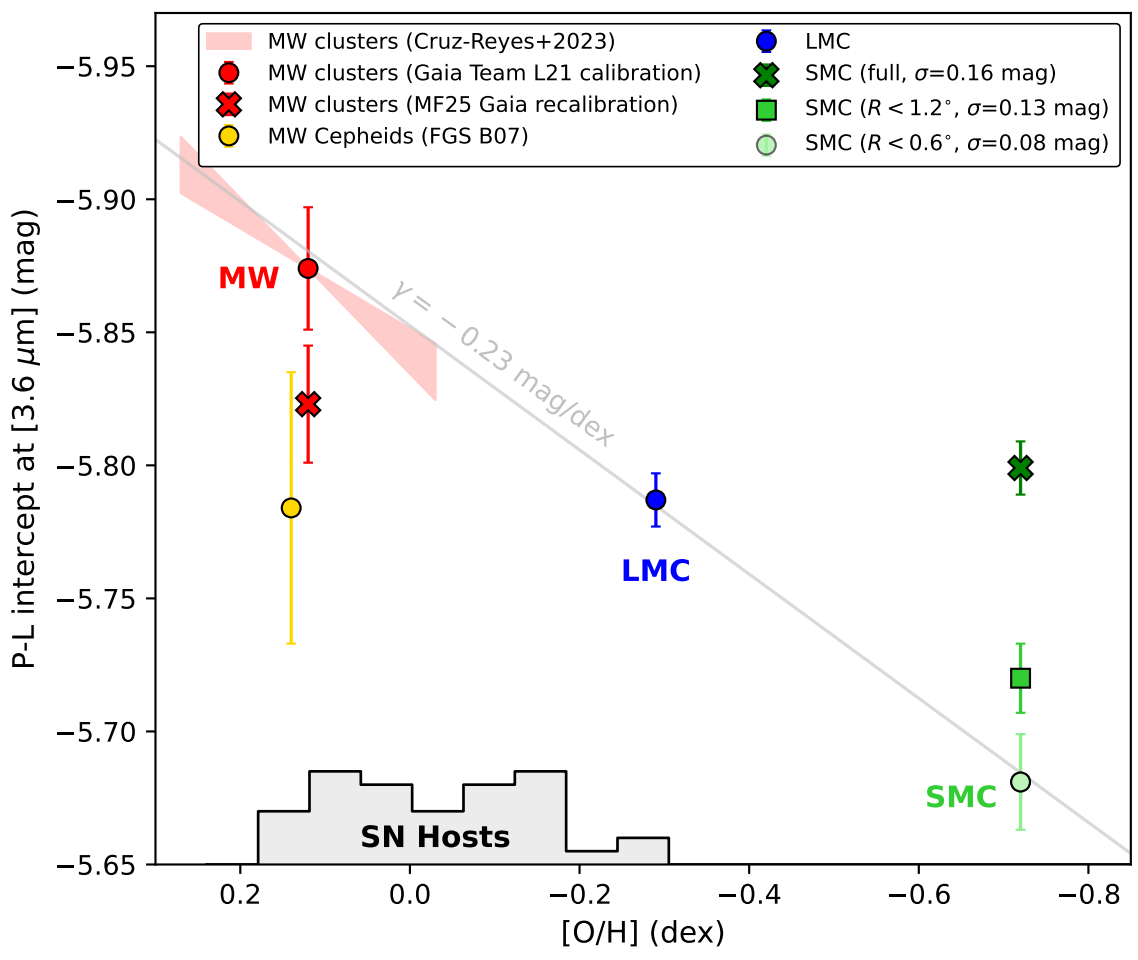


Figure 3. P–L intercept β , where $M=\alpha$ (log P-1) + β , in the [3.6 μ m] filter for Milky Way cluster Cepheids (red), the sample of 10 bright Cepheids with HST FGS parallaxes from B07 (yellow), LMC Cepheids (blue), and Cepheids in different regions of the SMC (green). The red "X" shows the P–L intercept obtained after the MF25 recalibration of Gaia EDR3 parallaxes. The metallicity on the horizontal axis is expressed in [O/H] for a direct comparison with abundances in SNIa host galaxies (gray histogram). The slope of the gray line represents a $\gamma \sim -0.23$ mag dex⁻¹ metallicity dependence obtained by fitting a straight line through the MW, LMC, and SMC. Conversely, the $\gamma \sim 0$ result by MF25 is obtained from a comparison between the MW red "X" marker, the LMC, and the SMC dark green "X" marker, which align with a horizontal line.

metallicity range covered by most of the more distant Type Ia supernova that calibrate host galaxies." However, the analysis presented in L. Breuval et al. (2021, 2022) covers the Milky Way, the LMC, and the SMC. As shown in Figure 3, the metallicity of Milky Way Cepheids is similar to (if not higher than) that of SNIa hosts, so there is no extrapolation needed.

2.4. A Differential Calibration of the Metallicity Effect between the LMC and the SMC

An independent approach for measuring the metallicity dependence γ comes from the comparison of Cepheids in the LMC and Small Magellanic Cloud (SMC) versus their geometric distance difference determined from DEBs. Section 4.2 of MF25 revisits this purely differential calibration of γ based on the metallicity difference between the LMC and SMC, and the difference in P–L intercept between the two galaxies in the [3.6 μ m] filter. The analysis follows the approach of P. Wielgórski et al. (2017), which yielded $\gamma \sim 0$ mag dex⁻¹ in the V, I, J, H, and K filters. However, the calibration of Cepheids with the geometric DEB distance is complicated by the well-known and substantial depth of the SMC (S. Subramanian & A. Subramaniam 2015; A. M. Jacyszyn-Dobrzeniecka et al. 2016; V. Scowcroft et al. 2016; V. Ripepi et al. 2017). L. Breuval et al. (2022, 2024)

analyzed the SMC P–L intercept and scatter as a function of the separation from the SMC core, found strong evolution of both, and concluded that these effects, attributed to the SMC's elongated shape, strongly affected the P. Wielgórski et al. (2017) result: applying a geometry correction (e.g., derived by D. Graczyk et al. 2020 from the planar distribution of the eclipsing binaries) to each Cepheid depending on their position, as well as using only Cepheids in the SMC 0.6 core region yields $\gamma \sim -0.15~{\rm mag~dex}^{-1}$, in good agreement with other empirical studies.

Here, we follow the same approach with the LMC and SMC Cepheid samples and the [3.6 μ m] photometry from V. Scowcroft et al. (2011, 2016) respectively. We assume $E(B-V)=0.07\pm0.01$ mag in the LMC and $E(B-V)=0.03\pm0.01$ in the SMC (D. M. Skowron et al. 2021) and we select Cepheids with P<60 days. In the SMC we use [Fe/H] = -0.785 ± 0.085 dex from M. Romaniello et al. (2025, in preparation). With a slope fixed to the LMC value of $\alpha=-3.31$, the P-L intercepts in the LMC and SMC are $\beta=-5.787\pm0.010$ and $\beta=-5.790\pm0.010$ mag, respectively. From Equation (7), we obtain an initial estimate of $\gamma=+0.008\pm0.037$ mag dex⁻¹, in agreement with MF25's claim. To account for the depth effects in the SMC, we now apply the geometry correction from L. Breuval et al. (2024)

Table 3
P–L Intercept β in the [3.6 μ m] Filter for the SMC Sample from V. Scowcroft et al. (2016) and Resulting Metallicity Dependence γ from the Differential Calibration with Respect to the LMC

Geometry Correction	Param.	R < 0.6 $(N = 21)$	$R < 1^{\circ}.2$ $(N = 41)$	Full $(N = 85)$	
No	$eta_{ ext{SMC}} \ \gamma \ \sigma_{ ext{PL}}$	$-5.665 \pm 0.016 \\ -0.323 \pm 0.090 \\ 0.089$	$-5.712 \pm 0.011 -0.198 \pm 0.063 0.131$	-5.790 ± 0.010 + 0.008 \pm 0.037 0.159	(mag) (mag dex ⁻¹) (mag)
Yes	$eta_{ ext{SMC}} \ \gamma \ \sigma_{ ext{PL}}$	$-5.673 \pm 0.016 \\ - 0.302 \pm 0.086 \\ 0.078$	$-5.693 \pm 0.011 \\ -0.249 \pm 0.072 \\ 0.127$	$-5.674 \pm 0.010 \\ -0.299 \pm 0.079 \\ 0.159$	(mag) (mag dex ⁻¹) (mag)

Note. We present the results for different regions around the SMC center, and with/without including geometry corrections. The P-L slope is fixed to -3.31 mag dex⁻¹. The initial calibration (full sample, no correction) and final result (R < 0.6, with corrections) are both highlighted in bold.

and we limit the sample to the SMC core region. The P-L intercept in the SMC and the resulting metallicity dependence γ are listed in Table 3 for the full sample, for R < 1.2 and R < 0.6, with and without the geometry corrections. The P-L intercepts obtained with geometry corrections are shown in Figure 3 in green. We see that the use of the SMC geometry and core region, independently corroborated by the tighter P-L dispersion, produce a value of $\gamma \sim -0.3~{\rm mag\,dex}^{-1}$, in better agreement with the canonical $\gamma \sim -0.2~{\rm mag\,dex}^{-1}$ from the literature. Finally, we note that P. Wielgórski et al. (2017) was based on the old SMC geometric distance by D. Graczyk et al. (2014), and that this measurement has been updated in D. Graczyk et al. (2020) with a larger sample of 15 eclipsing binaries. However, none of the recent studies by B. F. Madore & W. L. Freedman (2024a) and B. F. Madore et al. (2025a) use the modern value from D. Graczyk et al. (2020). This small difference of 0.027 mag in SMC distance modulus between D. Graczyk et al. (2014) and D. Graczyk et al. (2020) might affect γ at the $\sim 0.07 \,\mathrm{mag}\,\mathrm{dex}^{-1}$ level (assuming a 0.38 dex difference between the LMC and SMC).

To summarize, the case by MF25 for $\gamma\!\sim\!0$ between the LMC and the SMC requires (1) the use of an earlier DEB result from D. Graczyk et al. (2014) rather than the more recent D. Graczyk et al. (2020), (2) neglecting the SMC geometry described in D. Graczyk et al. (2020) and L. Breuval et al. (2024), and (3) neglecting strong and independent evidence that the SMC has significant depth effects that are largely if not fully resolved by limiting to the SMC core and application of the geometric model.

2.5. TRGB versus Cepheid Distance Moduli

Section 6 of MF25 presents a comparison between Cepheid and Tip of the Red Giant Branch (TRGB) distances across a large sample of galaxies. Based on the absence of a significant trend with host metallicity, the study concludes that $\gamma=0$. As previously discussed (see L. Breuval et al. 2024, Section 4.3), this approach presents challenges, as TRGB distances are not necessarily free from metallicity dependence (L. Rizzi et al. 2007; N. W. Koblischke & R. I. Anderson 2024). The TRGB data used in MF25 are drawn from disparate sources in the literature, despite the availability of recent and more uniformly measured samples (e.g., the Extragalactic Distance Database; R. B. Tully et al. 2009; G. S. Anand et al. 2021), which could potentially affect the outcome. Moreover, much of the leverage in the TRGB–Cepheid comparison comes from a small number of extremely metal-poor galaxies with sparse Cepheid

populations. These environments are rare in terms of spatial density, and the assumption that the few Cepheids present share the low average metallicity of their hosts may not be robust. It is more likely that these are high metallicity spots with some recent star formation, making it inappropriate to assume uniform low metallicity. In fact, the metallicities inferred for these Cepheids, around $[O/H] \sim -1.2$ dex, are lower than those found from direct measurements. For example, for the metal-poor galaxy Sextans A, MF25 assume $12 + \log(O/H) = 7.49$ dex from S. Sakai et al. (2004), equivalent to [O/H] = -1.2 dex. On the other hand, A. Kaufer et al. (2004) find [Fe/H] = -0.99 dex from high-resolution spectroscopy of supergiants, which is equivalent to [O/H] ~ -0.93 dex (the relationship $[O/H] \sim [Fe/H] + 0.06$ dex is adopted from A. G. Riess et al. 2022b), significantly less metal-poor. In contrast, direct geometric and spectroscopic measures of the most metal-poor Cepheids in the MW from the C-MetaLL project (E. Trentin et al. 2024) result in negative values of γ . Furthermore, A. Bhardwaj et al. (2024) used new homogeneous photometry and high-resolution spectroscopic metallicities for 61 Milky Way Cepheids and found that γ is more negative for metal-poor Cepheids (-1.1 < [Fe/H] <-0.3), which are more distant and have larger parallax uncertainties. The quality of the Cepheid data and the number of Cepheids in the metal-poor hosts used in MF25 is well below the measures in the better-studied LMC, SMC, and Milky Way. It is beyond the scope of this paper to investigate whether the abundances used in MF25 are representative of the Cepheids in the low-metallicity galaxies. However, it is important to note that mean abundances that apply to TRGB measurements may not be adequate for Cepheids, which are generally much younger. A further complication that can arise when going to the very low-metallicity regime is that the $[\alpha/\text{Fe}]$ ratios are no longer consistent between the samples, with α -enhancement simulating a higher metallicity (M. Salaris et al. 1993). This could have a significant impact on opacities, and hence, on a metallicity effect specified only relative to iron.

A specific example of this approach can be found in Section 4.2.2 of MF25, where a comparison of Cepheid (μ = 24.29 \pm 0.03 mag, W. L. Freedman et al. 2009), TRGB (μ = 24.30 \pm 0.03 mag, D. Hatt et al. 2017), and RR Lyrae (μ = 24.28 \pm 0.04 mag, D. Hatt et al. 2017) distance moduli to the metal-poor galaxy IC 1613 is presented. From the close agreement between the three values, they conclude that the metallicity dependence is consistent with zero. However, the MF25 sample, described as "well populated Cepheid P–L

relations," is actually based on only five Cepheids and each with single, random epoch observations in the Spitzer filters from W. L. Freedman et al. (2009). Given the intrinsic dispersion of $\sim\!0.08$ mag in the Spitzer P–L relation, the quoted uncertainty of ±0.03 mag in the Cepheid distance modulus may be underestimated. Moreover, a broader set of distance measurements in the literature, such as $\mu=24.20\pm0.07$ mag (A. Udalski et al. 2001), $\mu=24.29\pm0.03$ mag (G. Pietrzyński et al. 2006), $\mu=24.38\pm0.05$ mag (B. A. Jacobs et al. 2009, TRGB), and $\mu=24.31\pm0.06$ mag (A. E. Dolphin et al. 2001, RR Lyrae and Cepheids), suggests a wider spread among different estimates of the distance to IC 1613 than that considered in MF25. While these differences are mostly within $1\sigma\!-\!2\sigma$, they highlight the importance of accounting for measurement limitations and sample size when drawing conclusions about metallicity effects.

We further note that Figure 20 in MF25 highlights the L. Breuval et al. (2022) results in red and yellow, and the arrow near the Milky Way represents the MF25 parallax correction (in magnitude space). In this figure taken from B. F. Madore & W. L. Freedman (2024a) but later updated in B. F. Madore & W. L. Freedman (2024b), MF25 combine observations made in multiple wavelengths (the filter used to produce this plot is not specified), which invalidates the method due to inconsistent wavelength use. While the MF25 sample is described overall as "well observed galaxies," P-L relations often have <30 Cepheids and many of the metallicity measures are imprecise compared to the well-established values in the Milky Way, LMC, and SMC. Cepheid data are from 21 different sources, including before HST spherical aberration was fixed. The same trend can be found throughout the rest of the MF25 paper (see Appendix). For example, in Figure 21 in MF25, Cepheids in M33 come from a small sample of ground-based data from W. L. Freedman et al. (1991) rather than 154 Cepheids with HST observations in L. Breuval et al. (2023). In Figures 22 and 23 in MF25, residuals from extinction curve fits in SH0ES galaxies are taken from A. G. Riess et al. (2016) instead of the latter data release from A. G. Riess et al. (2022b). For the DEBs geometric distance to the SMC, MF25 cite D. Graczyk et al. (2014) and ignore the update by D. Graczyk et al. (2020). In contrast, the MW, LMC, and SMC Cepheids now have direct, spectroscopic metallicity measures, direct geometric distance measures, and uniform, high quality photometry from HST WFC3. It is therefore not surprising that inhomogeneous data wash out the signal that is seen with modern measurements. It is not clear why we should be limited to extracting results from such past data when there are more modern, better data sets available.

2.6. Residuals from the Milky Way Cepheid Sample

In Section 5, MF25 report that no correlation between P–L residuals and metallicity is found and characterize this conclusion as "not new," citing W. Narloch et al. (2023) in support. However, this interpretation does not align with the conclusions explicitly stated in W. Narloch et al. (2023). While that study does note the absence of a clear trend between residuals and metallicity in any band, including reddening-free Wesenheit analogs, it also emphasizes that the underlying metallicity range is narrow, limiting the ability to detect any potential trend. W. Narloch et al. (2023) state: "The comparison of the P–L/P–W relations residuals with metallicity does not show any clear trends in any band, but it should

Table 4
P–L Relation Scatter (in Mag) Quoted in MF25, Compared to the Actual Published Values in L. Breuval et al. (2021), L. Breuval et al. (2022), and B. F. Madore & W. L. Freedman (2012)

Band	MF25 (Table 3)	B21 (Table 1)	B22 (Table 4)	MF12 (Table 1)
\overline{V}	0.27	0.25	0.22	0.27
I	0.26	0.23	0.19	0.18
J	0.23	0.18	0.19	0.14
Н	0.22	0.17	0.18	0.12
K	0.20	0.17	0.17	0.11

Note. Values quoted by MF25 do not match the published ones and are systematically larger, making them look worse than they are.

be borne in mind that the range of metallicity used is rather narrow, and trends could possibly be revealed for a wider range of metallicities. Because of the small range of the metallicities of our Cepheids, we also decided not to investigate a period–luminosity-metallicity (PLZ) relation; however, such an analysis will be the subject of future projects." Additionally, the scatter values quoted in Table 3 of MF25, attributed to L. Breuval et al. (2021), do not match the values published in that work or in any of the related Breuval et al. papers, and also conflict the values from B. F. Madore & W. L. Freedman (2012; see Table 4). Therefore, the validity of these claims is questionable.

2.7. The Metallicity Dependence from Baade–Wesselink P–L Relations

In their Section 4.1, MF25 discuss the results by P. Fouqué et al. (2007) and J. Storm et al. (2011) based on Baade–Wesselink (BW) distances of Cepheids in the MW, LMC, and SMC. The latter work resulted in a small negative metallicity effect, which within errorbars can be interpreted as consistent with zero. However, a further update of these two works is presented in W. Gieren et al. (2018), based on an extended sample of Cepheids in the SMC (from N=5 to N=31 Cepheids), and was not mentioned in MF25. W. Gieren et al. (2018) used the exact same method as in J. Storm et al. (2011) and obtained a metallicity dependence between -0.22 and -0.33 mag dex $^{-1}$ for optical and near-infrared bands as well as W_{VI} and W_{JK} Wesenheit indices, with errors of \sim 0.15 mag dex $^{-1}$ in optical passbands and <0.1 mag dex $^{-1}$ for infrared bands and Wesenheit indices, which is fully consistent with the canonical -0.2 mag dex $^{-1}$ value.

In the BW method (W. Baade 1948; A. J. Wesselink 1946), the changes in the apparent angular diameter of the star, inferred from photometry and surface brightness—color relations, are compared to the physical radius displacement obtained from the integration of the velocity of the stellar atmosphere. The main source of uncertainty for BW distances is the value of the projection factor (*p*-factor) used to translate radial velocities measured from spectra into the true velocity of the stellar atmosphere. The precise value of this parameter, as well as its possible dependence with any physical parameter of the star, are still open questions (see B. Trahin et al. 2021, and references therein).

The large P–L scatter obtained from BW distances in J. Storm et al. (2011) and W. Gieren et al. (2018) is indeed high, as noted by MF25, and does not decrease with wavelength as expected. However, it does not rule out the

 Table 5

 Summary: Consequences of the Different Treatments of Gaia EDR3 Parallaxes

	Gaia Collaboration (L21)	B. F. Madore & W. L. Freedman (2025)
Distance to the Pleiades cluster	135 pc	120 pc
Parallax of distant quasars	\sim 0 μ as	\sim $-25~\mu{ m as}$
Inferred value of H_0	$73 \text{ km s}^{-1} \text{ Mpc}^{-1}$	$74.4 \text{ km s}^{-1} \text{ Mpc}^{-1}$

BW technique as unreliable, but rather indicates that the spread of the P-L relations is dominated by statistical errors on individual distance measurements, related not only to the poor knowledge of the p-factor, but also to the quality of photometry and radial velocities used in the analysis. In addition, as BW distances linearly depend on the assumed p-factor, any systematic shift of this parameter will not influence the measured relative distance modulus of the MW, LMC, and SMC Cepheids, which is the basis for the W. Gieren et al. (2018) calibration of the metallicity effect. Further, N. Nardetto et al. (2011) showed that the p-factor is largely independent of metallicity and I. B. Thompson et al. (2001) showed that the effect on surface brightness relations is also very small. Even though the BW method is not competitive with Gaia EDR3 parallaxes, the LMC distance modulus obtained by J. Storm et al. (2011) and W. Gieren et al. (2018) is in a excellent agreement with the geometric measurement from eclipsing binaries (G. Pietrzyński et al. 2019). Summing this up, regardless of the exact value (or period-dependence) of the p-factor, the results obtained from the BW method contradict the conclusions of MF25 and support a significant negative effect in the optical and near-infrared.

3. Consequences of the MF25 Recalibration of Gaia Parallaxes

The Gaia team, following L21, recommends a three-step calibration procedure: use Gaia EDR3 parallaxes, apply the L21 correction as a function of magnitude, color, and sky position, and, if applicable, solve for an additional additive offset tailored to specific source populations like Cepheids. In contrast, MF25 bypasses the L21 correction and introduces a fundamentally different, multiplicative correction that lacks justification within Gaia's parallax measurement framework. While this approach may yield similar results for cluster Cepheids, it will diverge significantly at other distances. Although MF25 do not explicitly state that their recalibration of Gaia parallaxes should be applied outside of their Cepheid sample, we demonstrate that applying the MF25 correction to other sources, such as the Pleiades or quasars, leads to inaccurate results, underscoring its lack of general validity. In particular, the Pleiades are cluster stars, and therefore the MF25 correction, derived for cluster Cepheids, would be expected to apply there. The consequences of the different treatments of Gaia parallaxes discussed in this paper are summarized in Table 5.

3.1. Distance to the Pleiades

The Pleiades is a very nearby open cluster, extensively studied in the Milky Way and much like the open clusters that host Cepheids farther away, so presumably the B. F. Madore & W. L. Freedman (2025) approach would apply to all open clusters. Here, we evaluate the impact of

the MF25 recalibration of Gaia cluster parallaxes for the Pleiades cluster distance. We recall that the MF25 recalibration relies on an additive 0.26 term in distance modulus, equivalent to a multiplicative correction in parallax space (Equations (1) and (2)). In the early 2000s, the Hipparcos astrometric mission measured a distance of 120 pc to the Pleiades (F. van Leeuwen 2009), which was proven to be too short by about 15 pc thanks to more precise measurements, including the recent Gaia parallaxes (Gaia Collaboration et al. 2016; G. Abramson 2018; N. Lodieu et al. 2019; J. Alfonso & A. García-Varela 2023). In addition, other methods independent from Gaia have confirmed the higher distance of about 135 pc using main-sequence fitting (S. M. Percival et al. 2005), HST FGS parallaxes (D. R. Soderblom et al. 2005), very long baseline radio interferometry (C. Melis et al. 2014), or stellar twins (T. Mädler et al. 2016). Applying the MF25 recalibration to Gaia EDR3 parallaxes for the Pleaides lowers their distance to \sim 120 pc (red point in Figure 4), similar to the Hipparcos measurement, and 15 pc shorter than the canonical value. It is interesting to note that the MF25 reliance on the HST FGS parallaxes to recalibrate Gaia EDR3 would produce conflicting results with the HST FGS measured parallax of the Pleiades, indicating that a multiplicative recalibration of Gaia parallaxes is inconsistent with a wider sample of HST FGS parallax measures. In fact, the L21 additive calibration would produce far better agreement to both sets of HST FGS parallaxes.

3.2. Nonzero Parallaxes of Quasars

The original Gaia EDR3 parallaxes are affected by a small systematic bias (L21) that varies across the sky and depends on magnitude, color, and position. On average, this bias is of the order of $\sim\!\!20\,\mu\rm as$ for quasars. This can be seen, for example, in the negative (hence unphysical^23) parallaxes measured for distant quasars, whose true parallaxes must be zero (see black points in Figure 5). Applying the L21 correction as an additive term to the parallaxes brings them back to zero within $\sim\!\!1\,\mu\rm as$ (blue points in Figure 5). In contrast, the recalibration proposed by MF25 multiplies Gaia EDR3 parallaxes by $\sim\!\!1.12$, which makes them even more negative—amplifying but not correcting the small, negative quasar parallaxes. The MF25 recalibration results in a systematic bias that cannot be reconciled with the known zero-parallax of quasars.

Negative Gaia parallaxes can be caused by errors in the observations. Even if a negative distance has no physical meaning, a certain number of stars are expected to have negative parallaxes from an error propagation perspective. The negative parallax tail is a useful diagnostic for the quality of the astrometric solution (F. Arenou et al. 2018; L. Lindegren et al. 2021b).

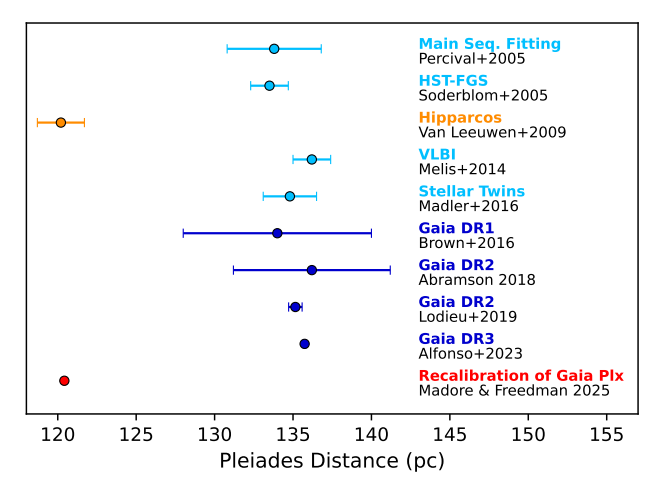


Figure 4. Distance estimates to the Pleiades open cluster. Light blue values are pre-Gaia measurements, orange is Hipparcos, dark blue are Gaia-based distances and the red point corresponds to Gaia EDR3 after applying the recalibration suggested by MF25.

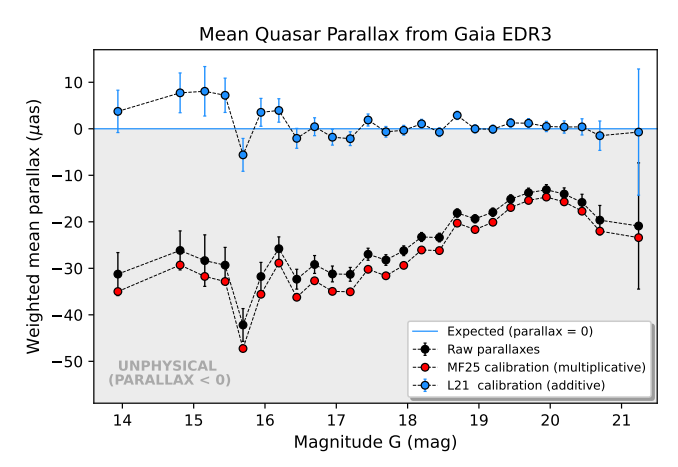


Figure 5. Mean parallaxes of distant quasars as a function of Gaia *G* magnitude from the Gaia EDR3 catalog without any correction (black), with the multiplicative correction proposed by MF25 (red) and with the additive correction recommended by the Gaia team (L21, in blue). Quasar parallaxes are expected to be equal to zero. Figure adapted from L21.

3.3. The Hubble Constant

The main result of the Key Project was a value of 72 km s⁻¹ Mpc⁻¹ for the Hubble constant, based on the LMC as only anchor and assuming $\gamma = -0.2 \text{ mag dex}^{-1}$ for the Cepheid metallicity dependence (W. L. Freedman et al. 2001). In that case, because the LMC is more metal-poor than SNIa host galaxies, the sensitivity of H_0 to the metallicity correction is important. W. L. Freedman et al. (2001) write: "The effect is systematic [..] if no correction for metallicity is applied, the value of H₀ is increased by $\sim 4\%$ ($\sim 3 \text{ km s}^{-1} \text{ Mpc}^{-1}$)." However, as stated in the Introduction, the impact of the Cepheid metallicity dependence γ for H_0 is now limited, thanks to the similarity in metallicity between Cepheids in anchor galaxies and in SNIa hosts. Although the LMC and SMC are particularly metal-poor, the use of the metal-rich Milky Way and NGC 4258 balances this difference (see Figure 21 in A. G. Riess et al. 2022b).

The MF25 recalibration of Gaia parallaxes applied to Cepheids in the Milky Way brings their P-L relation closer to that of the HST FGS B07 sample by 0.04 mag. This change

results in a less negative (i.e., larger, fainter) P–L intercept for Gaia Milky Way Cepheids, implying shorter distances to SNIa host galaxies, and thus a higher value for the Hubble constant. The MF25 correction would raise H_0 from the A. G. Riess et al. (2022a) Gaia calibration to 74.4 km s⁻¹ Mpc⁻¹. Similarly, A. G. Riess et al. (2016) used the HST FGS parallaxes from B07 to calibrate H_0 , resulting in 76 km s⁻¹ Mpc⁻¹, before the replacement of these with Gaia parallaxes (see Appendix B2 in A. G. Riess et al. 2022b). On the other hand, more recent distance ladders that include more metal-rich anchors like Gaia clusters (Riess et al. 2022, ApJ 938, 36) change the anchor-to-calibrator weighting to metal-rich so that $\gamma = 0$ can slightly lower H_0 by 0.4 km/s/Mpc H0DN Collaboration et al. (2025).

4. Discussion

In this paper, we revisited the recalibration of Gaia EDR3 parallaxes proposed in MF25. We first reproduced the cluster Cepheid P-L relation as presented in that work, and then replaced the 0.26 mag magnitude offset proposed by MF25 (equivalent to a multiplicative parallax correction) with the additive parallax offset ϖ_{L21} recommended by the Gaia team (L. Lindegren et al. 2021a). This substitution changes the Cepheid metallicity dependence γ from \sim 0 to $-0.16 \text{ mag dex}^{-1}$, bringing it into close agreement with both widely adopted empirical values and predictions from stellar models. We also examined additional methods employed in MF25, including the comparison of P-L relations in the LMC and SMC. Using an updated treatment of the SMC geometry and limiting the Cepheid sample to the SMC core region, we find that this approach likewise supports a negative metallicity dependence. We further note limitations in the use of Cepheid-TRGB distance comparisons as a test of γ , which we show does not provide a reliable test of the metallicity dependence at the fidelity of what can be directly measured from the best LMC, SMC, and MW data. Finally, we assess the broader implications of the MF25 Gaia parallax recalibration and find that it leads to several inconsistencies: notably, a distance many σ too short for the Pleiades cluster, and negative and unphysical parallaxes for extragalactic quasars.

It is likely that the upcoming Gaia DR4, based on several more years of data and with improvements in the focal plane calibration, will reduce or remove the dependence of the Gaia parallax offset on stellar properties and location, thereby obviating the need for an additional parallax correction for bright Cepheids. This would result in a significant improvement in the calibration of the period–luminosity relation for Milky Way Cepheids, and a reduction of any residual systematic uncertainties.

The metallicity dependence is a small effect that has a mild impact on the value of the Hubble constant. As it remains difficult to measure its value, a precise determination therefore requires using the highest-quality data, as well as taking into account possible α -enhancement effects in the metal-poor regime, since results will otherwise remain inconclusive or incorrect, especially if systematics cannot be fully understood or quantified. We conclude that the best available data consistently supports a nonzero, negative (i.e., metal-rich Cepheids are brighter at fixed period), metallicity dependence.

Acknowledgments

We are grateful to Lennart Lindegren for providing the quasar parallax data to produce Figure 5 and for his insightful comments on the paper. L.B. would like to thank Paule Sonnentrucker, Chris Evans, Boris Trahin, Laura Herold, and Yukei Murakami for their continuous support. This project has received funding from the European Research Council (ERC) under the European Union's Horizon 2020 research and innovation program (grant Agreement No. 947660). R.I.A., M. C.R., and S.K. are funded by the Swiss National Science Foundation through an Eccellenza Professorial Fellowship (award PCEFP2_194638). G.D.S. acknowledges funding from the INAF-ASTROFIT fellowship, from Gaia DPAC through INAF and ASI (PI: M.G. Lattanzi), and from INFN (Naples Section) through the QGSKY and Moonlight2 initiatives. A.B. is thankful for funding from the Anusandhan National Research Foundation (ANRF) under the Prime Minister Early Career Research Grant scheme (ANRF/ECRG/2024/ 000675/PMS). This research has received funding from the European Research Council under the the Horizon 2020 research and innovation program (project UniverScale, grant agreement 951549). This work has been supported by the Polish-French Marie Skłodowska-Curie and Pierre Curie Science Prize awarded by the Foundation for Polish Science. The authors acknowledge the support of the French Agence Nationale de la Recherche (ANR), under grant ANR-23-CE31-0009-01 (Unlock-pfactor). V.R., M.M., and E.T. acknowledge funding from INAF GO-GTO grant 2023 "C-MetaLL-Cepheid metallicity in the Leavitt law" (P.I. V. Ripepi). This research was supported by the International Space Science Institute (ISSI) in Bern/Beijing through ISSI/ISSI-BJ International Team project ID #24-603—"EXPANDING Uni-(EXploiting Precision AstroNomical Distance INdicators in the Gaia Universe), and by the International Space Science Institute (ISSI) in Bern, through ISSI International Team Project #490, "SH0T: The Stellar Path to the H_0 Tension in the Gaia, TESS, LSST and JWST Era" (PI: G. Clementini).

Appendix Choice of Data

Table 6 shows a comparison between the data adopted in MF25 and the best available data.

Table 6
Data Adopted in MF25 Compared to the Best Available Data

		MF25	Best Available
Pulsation period for V367 Sct	MF25 Table 1	B. F. Madore & S. van den Bergh (1975) $\log P = 0.721$	M. Cruz Reyes & R. I. Anderson (2023) $\log P = 0.799$
Number of SMC Cepheids with BW distances	MF25 Section 4.1.2	J. Storm et al. (2011) $N = 5$	W. Gieren et al. (2018) N = 31
Number of DEBs for	MF25	D. Graczyk et al. (2014) $N = 5$	D. Graczyk et al. (2020)
SMC geometric distance	Section 8		N = 15
Number of SNIa host galaxies for residuals of extinction curve fits	MF25	A. G. Riess et al. (2016)	A. G. Riess et al. (2022b)
	Figures 22, 23	N = 19	N = 37
Number of Cepheids	MF25	M. Marconi et al. (2017)	L. Breuval et al. (2024)
in SMC	Section 6	N = 9 (ground)	N = 87 (HST)
Number of Cepheids	MF25	C. S. Kochanek (1997) N = 30 (ground)	S. Li et al. (2021)
in M31	Section 6		N = 55 (HST)
Number of Cepheids in M33	MF25 Section 6	W. L. Freedman et al. (1991) N = 10 (ground)	L. Breuval et al. (2023) N = 154 (HST)
Number of Cepheids	MF25	G. Piotto et al. (1994)	A. E. Dolphin et al. (2003)
in Sextans A	Section 6	N = 7 (ground)	N = 82 (HST)
Number of Cepheids	MF25	P. B. Stetson et al. (1998)	A. G. Riess et al. (2022b)
in M101	Section 6	N = 61	N = 260
Number of Cepheids	MF25	A. G. Riess et al. (2016)	W. Yuan et al. (2022)
in NGC 4258	Section 6	N = 141	N = 669

ORCID iDs

Louise Breuval https://orcid.org/0000-0003-3889-7709 Gagandeep S. Anand https://orcid.org/0000-0002-5259-2314 Richard I. Anderson https://orcid.org/0000-0001-

Richard I. Anderson https://orcid.org/0000-0001-8089-4419

Rachael Beaton https://orcid.org/0000-0002-1691-8217
Anupam Bhardwaj https://orcid.org/0000-0001-6147-3360
Gisella Clementini https://orcid.org/0000-0001-9206-9723
Mauricio Cruz Reyes https://orcid.org/0000-0003-2443-173X

Caroline D. Huang https://orcid.org/0000-0001-6169-8586
Pierre Kervella https://orcid.org/0000-0003-0626-1749
Saniya Khan https://orcid.org/0000-0001-5998-5885
Lucas M. Macri https://orcid.org/0000-0002-1775-4859
Marcella Marconi https://orcid.org/0000-0002-1330-2927
Javier H. Minnit https://orcid.org/0000-0002-6342-0331
Adam G. Riess https://orcid.org/0000-0002-6124-1196
Vincenzo Ripepi https://orcid.org/0000-0003-1801-426X
Martino Romaniello https://orcid.org/0000-0002-5527-6317

Daniel Scolnic https://orcid.org/0000-0002-4934-5849
Erasmo Trentin https://orcid.org/0000-0002-3899-566X
Piotr Wielgórski https://orcid.org/0000-0002-1662-5756
Wenlong Yuan https://orcid.org/0000-0001-9420-6525

References

```
Abramson, G. 2018, RNAAS, 2, 150
Alfonso, J., & García-Varela, A. 2023, A&A, 677, A163
Anand, G. S., Rizzi, L., Tully, R. B., et al. 2021, AJ, 162, 80
Anderson, R. I., Eyer, L., & Mowlavi, N. 2013, MNRAS, 434, 2238
Anderson, R. I., Saio, H., Ekström, S., Georgy, C., & Meynet, G. 2016, A&A,
  591, A8
Arenou, F., Luri, X., Babusiaux, C., et al. 2018, A&A, 616, A17
Baade, W. 1948, PASP, 60, 230
Benedict, G. F., McArthur, B. E., Feast, M. W., et al. 2007, AJ, 133, 1810
Bhardwaj, A., Rejkuba, M., de Grijs, R., et al. 2021, ApJ, 909, 200
Bhardwaj, A., Riess, A. G., Catanzaro, G., et al. 2023, ApJL, 955, L13
Bhardwaj, A., Ripepi, V., Testa, V., et al. 2024, A&A, 683, A234
Bono, G., Caputo, F., Cassisi, S., et al. 2000a, ApJ, 543, 955
Bono, G., Castellani, V., & Marconi, M. 2000b, ApJ, 529, 293
Bono, G., Marconi, M., & Stellingwerf, R. F. 1999, ApJS, 122, 167
Breuval, L., Kervella, P., Anderson, R. I., et al. 2020, A&A, 643, A115
Breuval, L., Kervella, P., Wielgórski, P., et al. 2021, ApJ, 913, 38
Breuval, L., Riess, A. G., Casertano, S., et al. 2024, ApJ, 973, 30
Breuval, L., Riess, A. G., Kervella, P., Anderson, R. I., & Romaniello, M.
   2022, ApJ, 939, 89
Breuval, L., Riess, A. G., Macri, L. M., et al. 2023, ApJ, 951, 118
Cantat-Gaudin, T., Anders, F., Castro-Ginard, A., et al. 2020, A&A, 640, A1
Castellani, V., Chieffi, A., & Straniero, O. 1992, ApJS, 78, 517
Castro-Ginard, A., Jordi, C., Luri, X., et al. 2022, A&A, 661, A118
Cruz Reyes, M., & Anderson, R. I. 2023, A&A, 672, A85
De Somma, G., Marconi, M., Molinaro, R., et al. 2022, ApJS, 262, 25
Dolphin, A. E., Saha, A., Skillman, E. D., et al. 2001, ApJ, 550, 554
Dolphin, A. E., Saha, A., Skillman, E. D., et al. 2003, AJ, 125, 1261
Fabricius, C., Luri, X., Arenou, F., et al. 2021, A&A, 649, A5
Fiorentino, G., Caputo, F., Marconi, M., & Musella, I. 2002, ApJ, 576, 402
Fouqué, P., Arriagada, P., Storm, J., et al. 2007, A&A, 476, 73
Freedman, W. L., & Madore, B. F. 2011, ApJ, 734, 46
Freedman, W. L., Madore, B. F., Gibson, B. K., et al. 2001, ApJ, 553, 47
Freedman, W. L., Rigby, J., Madore, B. F., et al. 2009, ApJ, 695, 996
Freedman, W. L., Wilson, C. D., & Madore, B. F. 1991, ApJ, 372, 455
Gaia Collaboration, Brown, A. G. A., Vallenari, A., et al. 2016, A&A, 595, A2
Gaia Collaboration, Brown, A. G. A., Vallenari, A., et al. 2021, A&A, 649, A1
```

```
Gallenne, A., Evans, N. R., Kervella, P., et al. 2025, A&A, 693, A111
Gieren, W., Storm, J., Konorski, P., et al. 2018, A&A, 620, A99
Graczyk, D., Pietrzyński, G., Thompson, I. B., et al. 2014, ApJ, 780, 59
Graczyk, D., Pietrzyński, G., Thompson, I. B., et al. 2020, ApJ, 904, 13
Groenewegen, M. A. T. 2021, A&A, 654, A20
H0DN Collaboration, Casertano, Stefano, Anand, Gagandeep, et al. 2025,
   arXiv:2510.23823
Hatt, D., Beaton, R. L., Freedman, W. L., et al. 2017, ApJ, 845, 146
Huang, Y., Yuan, H., Beers, T. C., & Zhang, H. 2021, ApJL, 910, L5
Hunt, E. L., & Reffert, S. 2023, A&A, 673, A114
Jacobs, B. A., Rizzi, L., Tully, R. B., et al. 2009, AJ, 138, 332
Jacyszyn-Dobrzeniecka, A. M., Skowron, D. M., Mróz, P., et al. 2016, AcA,
   66, 149
Kaufer, A., Venn, K. A., Tolstoy, E., Pinte, C., & Kudritzki, R.-P. 2004, AJ,
   127, 2723
Kennicutt, R. C. J., Stetson, P. B., Saha, A., et al. 1998, ApJ, 498, 181
Khan, S., Anderson, R. I., Ekström, S., Georgy, C., & Breuval, L. 2025,
                           cs, 702, A235
Khan, S., Anderson, R. I., Miglio, A., Mosser, B., & Elsworth, Y. P. 2023,
   A&A, 680, A105
Kharchenko, N. V., Piskunov, A. E., Schilbach, E., Röser, S., & Scholz, R. D.
   2013, A&A, 558, A53
Koblischke, N. W., & Anderson, R. I. 2024, ApJ, 974, 181
Kochanek, C. S. 1997, ApJ, 491, 13
Li, S., Riess, A. G., Busch, M. P., et al. 2021, ApJ, 920, 84
Lindegren, L., Bastian, U., Biermann, M., et al. 2021a, A&A, 649, A4
Lindegren, L., Klioner, S. A., Hernández, J., et al. 2021b, A&A, 649, A2
Lodieu, N., Pérez-Garrido, A., Smart, R. L., & Silvotti, R. 2019, A&A,
Mädler, T., Jofré, P., Gilmore, G., et al. 2016, A&A, 595, A59
Madore, B. F., & Freedman, W. L. 2012, ApJ, 744, 132
Madore, B. F., & Freedman, W. L. 2024a, ApJ, 961, 166
Madore, B. F., & Freedman, W. L. 2024b, ApJ, 970, 193
Madore, B. F., & Freedman, W. L. 2025, ApJ, 983, 161
Madore, B. F., Freedman, W. L., Hoyt, T., et al. 2025a, AJ, 169, 162
Madore, B. F., Freedman, W. L., & Owens, K. 2025b, ApJ, 981, 32
Madore, B. F., Stobie, R. S., & van den Bergh, S. 1978, MNRAS, 183, 13
Madore, B. F., & van den Bergh, S. 1975, ApJ, 197, 55
Maíz Apellániz, J., Pantaleoni González, M., & Barbá, R. H. 2021, A&A,
   649, A13
Marconi, M., Molinaro, R., Ripepi, V., et al. 2017, MNRAS, 466, 3206
Marconi, M., Musella, I., & Fiorentino, G. 2005, ApJ, 632, 590
Melis, C., Reid, M. J., Mioduszewski, A. J., Stauffer, J. R., & Bower, G. C.
   2014, Sci, 345, 1029
Monson, A. J., Freedman, W. L., Madore, B. F., et al. 2012, ApJ, 759, 146
Nardetto, N., Fokin, A., Fouqué, P., et al. 2011, A&A, 534, L16
Narloch, W., Hajdu, G., Pietrzyński, G., et al. 2023, ApJ, 953, 14
Owens, K. A., Freedman, W. L., Madore, B. F., & Lee, A. J. 2022, ApJ, 927, 8
Percival, S. M., Salaris, M., & Groenewegen, M. A. T. 2005, A&A, 429, 887
Pietrzyński, G., Gieren, W., Soszyński, I., et al. 2006, ApJ, 642, 216
Pietrzyński, G., Graczyk, D., Gallenne, A., et al. 2019, Natur, 567, 200
Piotto, G., Capaccioli, M., & Pellegrini, C. 1994, A&A, 287, 371
Ren, F., Chen, X., Zhang, H., et al. 2021, ApJL, 911, L20
Riess, A. G., Breuval, L., Yuan, W., et al. 2022a, ApJ, 938, 36
Riess, A. G., Casertano, S., Yuan, W., et al. 2021, ApJL, 908, L6
Riess, A. G., Macri, L. M., Hoffmann, S. L., et al. 2016, ApJ, 826, 56
Riess, A. G., Yuan, W., Macri, L. M., et al. 2022b, ApJL, 934, L7
Ripepi, V., Catanzaro, G., Clementini, G., et al. 2022, A&A, 659, A167
Ripepi, V., Cioni, M.-R. L., Moretti, M. I., et al. 2017, MNRAS, 472, 808
Ripepi, V., Clementini, G., Molinaro, R., et al. 2023, A&A, 674, A17
Rizzi, L., Tully, R. B., Makarov, D., et al. 2007, ApJ, 661, 815
Romaniello, M., Riess, A., Mancino, S., et al. 2022, A&A, 658, A29
Sakai, S., Ferrarese, L., Kennicutt, R. C. J., & Saha, A. 2004, ApJ, 608, 42
Salaris, M., Chieffi, A., & Straniero, O. 1993, ApJ, 414, 580
Scowcroft, V., Freedman, W. L., Madore, B. F., et al. 2011, ApJ, 743, 76
Scowcroft, V., Freedman, W. L., Madore, B. F., et al. 2012, ApJ, 747, 84
Scowcroft, V., Freedman, W. L., Madore, B. F., et al. 2016, ApJ, 816, 49
Skowron, D. M., Skowron, J., Udalski, A., et al. 2021, ApJS, 252, 23
Soderblom, D. R., Nelan, E., Benedict, G. F., et al. 2005, AJ, 129, 1616
Stassun, K. G., & Torres, G. 2021, ApJL, 907, L33
Stetson, P. B., Saha, A., Ferrarese, L., et al. 1998, ApJ, 508, 491
Storm, J., Gieren, W., Fouqué, P., et al. 2011, A&A, 534, A95
Subramanian, S., & Subramaniam, A. 2015, A&A, 573, A135
Thompson, I. B., Kaluzny, J., Pych, W., et al. 2001, AJ, 121, 3089
Trahin, B., Breuval, L., Kervella, P., et al. 2021, A&A, 656, A102
Trentin, E., Ripepi, V., Molinaro, R., et al. 2024, A&A, 681, A65
```

Tully, R. B., Rizzi, L., Shaya, E. J., et al. 2009, AJ, 138, 323
Turner, D. G., van den Bergh, S., Younger, P. F., Danks, T. A., & Forbes, D. 1993, ApJS, 85, 119
Udalski, A., Wyrzykowski, L., Pietrzynski, G., et al. 2001, AcA, 51, 221
van Leeuwen, F. 2009, A&A, 497, 209
Vasiliev, E., & Baumgardt, H. 2021, MNRAS, 505, 5978

Wang, H., Xu, Y., Lin, Z., et al. 2024, AJ, 168, 34 Wesselink, A. J. 1946, BAN, 10, 91 Wielgórski, P., Pietrzyński, G., Gieren, W., et al. 2017, ApJ, 842, 116 Yuan, W., Macri, L. M., Riess, A. G., et al. 2022, ApJ, 940, 64 Zhou, X., & Chen, X. 2021, MNRAS, 504, 4768 Zinn, J. C. 2021, AJ, 161, 214